Eur. Phys. J. D **43**, 229–232 (2007)
DOI: 10.1140/epjd/e2007-00103-0

**THE EUROPEAN
PHYSICAL JOURNAL D**

Optical and photoelectron spectroscopic studies of alkyl-passivated silicon nanoparticles

A. Tanaka[a], R. Saito, T. Kamikake, M. Imamura, and H. Yasuda

Department of Mechanical Engineering, Faculty of Engineering, Kobe University, Nada-ku, Kobe 657-8501, Japan

Received 25 July 2006 / Received in final form 8 September 2006

Abstract. We have performed the optical and photoelectron spectroscopic studies of alkyl-passivated Si nanoparticles synthesized by a solution route. The alkyl-passivated Si nanoparticle with mean diameter less than about 2 nm exhibits a strong ultraviolet-blue photoluminescence. Furthermore, we have directly investigated their electronic structures in the vicinity of Fermi level by means of valence-band photoemission measurements using synchrotron radiation. From these results, the detailed optical properties and electronic structures of alkyl-passivated Si nanoparticles are discussed.

PACS. 78.67.-n Optical properties of low-dimensional, mesoscopic, and nanoscale materials and structures – 78.67.Bf Nanocrystals and nanoparticles – 73.22.-f Electronic structure of nanoscale materials: clusters, nanoparticles, nanotubes, and nanocrystals

1 Introduction

Physical and optical properties of semiconductor nanoparticles have received extensive interest in recent years [1]. Especially, the various Si nanoparticles are attracting much interest from the viewpoint of both fundamental and device physics, since it has been reported that they show a strong photoluminescence (PL) [2] and therefore it is suggested that these Si nanoparticles could be important constituents of future photonics devices. While a large number of works focused on the optical properties of Si nanoparticles prepared by the various methods, such as chemical etching, ion sputtering, chemical vapor deposition, ion implantation, and laser ablation, etc. [3–7], have been reported to date, these optical properties depend on the samples in the literatures and are ascribed to various processes such as quantum confinement, oxide-related species, surface state, molecular species, or impurities, etc. Therefore, the interplay between the intrinsic quantum confinement effects and extrinsic surface/interface related effects is still controversial. Since most of the previous works have concentrated on only their optical spectra and have indirectly discussed their electronic structures from the results of optical measurements, the discussions regarding their optical properties are considered to be still unclear. In order to understand the intrinsic properties of Si nanoparticles, it is indispensable to prepare the samples with well-defined surface and to directly characterize their intrinsic electronic structures. In this work, we have synthesized the alkyl-passivated Si nanoparticles with well-crystalline nature and well-passivated surface by the chemical solution routes, and have directly characterized their electronic structures in the vicinity of Fermi level by means of photoelectron spectroscopy using synchrotron radiation as well as their optical properties. From these results, we will discuss the correlation between their optical properties and electronic structures of well-defined surface-passivated Si nanoparticles.

2 Experiment

The *n*-butyl-passivated Si nanoparticles used in this work were synthesized by the oxidation of magnesium silicide (Mg_2Si) with bromine and the subsequent passivation of the Si_mBr product (Br-capped Si nanoparticle) with use of an butyllithium reagent. Subsequently, we carried out the size-selective ultrafiltration treatments for thus synthesized Si nanoparticles in order to improve the size distribution. The detailed procedures is described elsewhere [8]. The size distributions in diameter of the synthesized Si nanoparticles were characterized by ex-situ observations with transmission electron microscope (TEM). Fourier transform infrared (FTIR), PL and PL excitation (PLE) spectra were measured at room temperature in order to characterize their chemical states and optical properties. In order to directly investigate their electronic structures, the photoemission measurements using synchrotron radiation were carried out at BL-5U of UVSOR-II Facility, Institute for Molecular Science, Okazaki, Japan. For the synchrotron-radiation photoemission measurements, the synthesized *n*-butyl-passivated Si nanoparticles were supported on the highly oriented pyrolytic graphite (HOPG) substrates by evaporating the solvent (hexane) from the dispersion of *n*-butyl-passivated Si nanoparticles on the single-crystalline

---

[a] e-mail: `a-tanaka@mech.kobe-u.ac.jp`

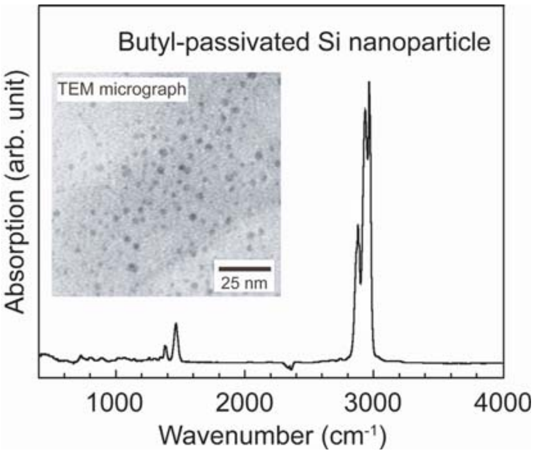

Fig. 1. FTIR spectrum of n-butyl-passivated Si nanoparticle after size-selective ultrafiltration treatment (with mean diameter less than about 2 nm). The inset shows the TEM micrograph.

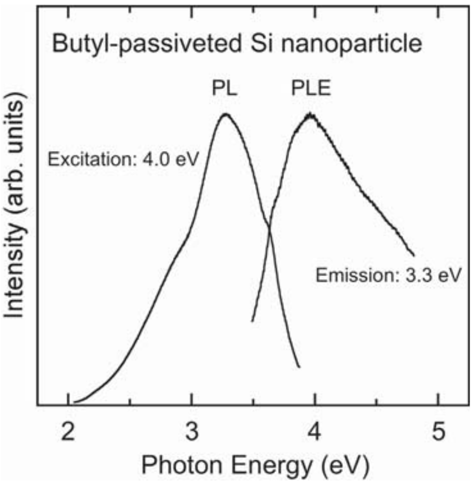

Fig. 2. Maximum PL and PLE spectra of n-butyl-passivated Si nanoparticle with mean diameter less than about 2 nm. PL spectrum is measured with excitation energy of 4 eV, and PLE spectrum is measured at emission energy of 3.3 eV.

HOPG cleaved surface in a nitrogen-filled glove bag directly connected to the ultrahigh-vacuum photoelectron spectrometer. Then the samples were transferred into the photoemission analysis chamber without exposure to air. Photoemission measurements were performed at room temperature with incident photon energy of 184 eV. In order to prevent synchrotron-radiation irradiation damage, the synchrotron-radiation intensity was reduced such that the photoemission spectra showed no change in the course of the measurements.

3 Results and discussion

Figure 1 shows the FTIR spectrum and TEM micrograph of n-butyl-passivated Si nanoparticles after size-selective ultrafiltration treatment, respectively. From the TEM micrograph, it is found that the mean diameter of the sample after ultrafiltration treatment has been estimated to be less than about 2 nm. Moreover, this TEM micrograph shows that each n-butyl-passivated Si nanoparticle is well separated from its neighboring nanoparticles, indicating that the present Si nanoparticles are well surface-passivated by butyl molecules. On the other hand, high-resolution TEM micrograph (not give here) of the present Si nanoparticles show the identical lattice fringes to bulk Si crystallite, indicative of well crystalline nature. As shown in Figure 1, FTIR spectrum of the present Si nanoparticles exhibits the spectral features around 2870–2960 cm^{-1} and 1360–1460 cm^{-1} wavenumbers. The spectral features around 2870–2960 cm^{-1} wavenumbers originate from methylene and terminated methyl stretching modes, and those around 1360–1460 cm^{-1} wavenumbers originate from methylene and terminated methyl deformation and/or scissor modes. These vibration modes are attributed to the surface passivants of butyl chains. An important point to note is that no spectral features around 1000–1100 cm^{-1} wavenumber, attributed to Si-O stretching modes, has been observed. This indicates no oxygen contamination on the surface of Si nanoparticle and no Si-O containing impurity in the Si nanoparticle. From these results of FTIR measurement, it is confirmed that the present Si nanoparticles are perfectly surface-passivated by n-butyl molecules and have no surface contamination and impurity.

Figure 2 shows the maximum PL and the corresponding PLE spectra measured at room temperature of n-butyl-passivated Si nanoparticle with mean diameter less than about 2 nm after ultrafiltration treatment. Maximum PL spectrum of the present Si nanoparticles exhibit the distinct emission around 3.3 eV in photon energy and no emission in the photon energy region below 2 eV. Moreover, the monotonic shift of this emission as a function of excitation photon energy is observed. The corresponding PLE spectrum exhibits the distinct resonance around 4 eV in photon energy, and the monotonic shift of this resonance as a function of emission photon energy is also observed. These resonance energies in the PLE spectra are significantly larger than bulk Si band gap energy. Since PL derived from the surface-passivant molecules and/or trap states will show no excitation photon energy dependence, it is considered that the present ultraviolet-blue PL from the n-butyl-passivated Si nanoparticle is not related to the surface-passivant molecules and/or trap states such as oxide and/or defect/impurity sites. Another possibility of the origin of the present ultraviolet-blue PL is the quantum confinement effect in the Si nanoparticle with decreasing the nanoparticle size. If the quantum confinement effect is revealed in the present Si nanoparticle, the energy gap of each Si nanoparticle will depend on the nanoparticle size. Since even sample after size-selective ultrafiltration treatment have a finite size distribution as shown in Figure 1, it is considered that the monotonic shift of PL as a function of excitation

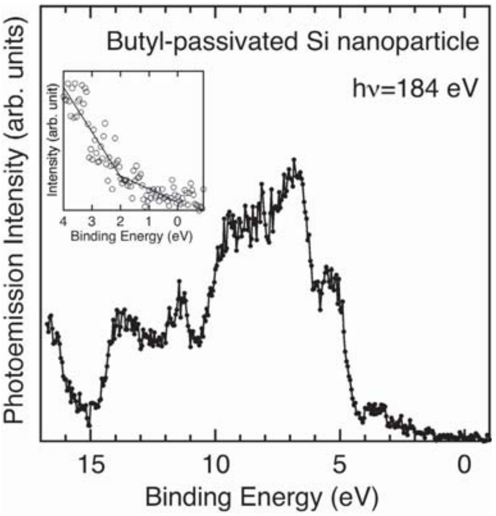

Fig. 3. Valence-band photoemission spectrum of *n*-butyl-passivated Si nanoparticles with mean diameter less than about 2 nm supported on the HOPG substrate at room temperature measured with photon energy of 184 eV using synchrotron radiation. The inset shows the photoemission spectrum in the vicinity of Fermi level.

photon energy originates from the selective excitation of Si nanoparticles with different sizes that have different optical transition energies. That is, the present ultraviolet-blue PL observed for *n*-butyl-passivated Si nanoparticles is considered to originate from electron-hole pair recombination between the modified conduction-band (LUMO) and valence-band (HOMO) due to the quantum size effect.

In order to directly investigate their electronic structures, we have carried out the photoemission study using synchrotron radiation. Figure 3 shows the valence-band photoemission spectrum of the present Si nanoparticle on the HOPG substrate with photon energy of 184 eV. Previously, the photoemission spectrum of methyl-terminated Si(111) surface and the cluster calculations by DV-Xα method have been reported by Miyadera et al. [9] From the analogy with the result of methyl-terminated Si(111) surface, the spectral features around 7 and 5.5 eV in binding energies originate from the C 2*p* derived states. The spectral feature around 7 eV binding energy originate from the C-H bonds in the butyl surface-passivants, and that around 5.5 eV binding energy originate from the σ_{Si-C} bonds between Si nanoparticle and butyl surface-passivants. The spectral features around 3.5, 9, and 11.5 eV in binding energies originate from the Si 3*s*- and 3*p*-derived electronic states. The additional feature around 13.5 eV in binding energy corresponds to that derived from HOPG substrate, since there is an uncovered region of Si nanoparticles on the HOPG substrate in the present measurement. In the inset of Figure 3, we plot the photoemission spectrum in the vicinity of Fermi level on an expanded energy scale. The spectral intensity from the HOPG substrate, which reflects the vanishing semimetallic density of states toward the Fermi level, contributes to the photoemission spectrum in the vicinity of Fermi level, but no contribution of C 2*s*- and 2*p*-derived states from butyl molecular orbitals appears in this energy region. Therefore, it is considered that the additional steep slope on the linear background signal (spectral feature from the HOPG substrate) originates from the valence-band structure of the present *n*-butyl-passivated Si nanoparticles. As shown in the inset of Figure 3, we have estimated the valence-band maximum (HOMO) energy from an intersection point of two lines extrapolated by the least squares method of spectral tail derived from the valence-band structure of Si nanoparticles and the background signal from the HOPG substrate. From this analysis, we obtain the valence-band maximum of about 2 eV below the Fermi level. If the Fermi level is considered to be located in the middle of energy gap (HOMO-LUMO gap), the energy gap of the present Si nanoparticles can be estimated to about 4 eV. This value is consistent with the resonance energies in the PLE spectra fairly well. Therefore, it is confirmed that the PL from the present *n*-butyl-passivated Si nanoparticles originate from the electron-hole pair recombination between the modified conduction-band (LUMO) and valence-band (HOMO) due to the quantum size effect.

Puzder et al. [10] have reported the surface chemical-state dependence of the electronic structures of hydrogen-passivated Si nanoparticles by means of quantum Monte Carlo calculations. They have shown that the significant changes in the HOMO-LUMO gap when the surface contains passivants other than hydrogen, in particular atomic oxygen. For example, HOMO-LUMO gap of fully hydrogen-passivated Si nanoparticle with relevant size regime to the present Si nanoparticle is about 4 eV, but that of Si nanoparticle with multiple oxygen contamination is reduced to about 2 eV. In fact, alkyl/alkoxy-passivated Si nanoparticles show that the oxygen contamination induces the red shift of PL [11]. Moreover, Reboredo et al. [12] have recently reported the results of ab initio calculations using density functional theory for the various surface-passivated Si nanoparticles. They have calculated the surface-passivant dependence of HOMO-LUMO gaps of surface-passivated Si nanoparticles, and have concluded that HOMO-LUMO gap is weakly affected as a function of surface passivation, in particular when the Si-H bond (that is, perfectly hydrogen-passivated Si nanoparticle) is replaced by a Si-C bond (that is, perfectly alkyl-passivated Si nanoparticle). From the comparison with these previous theoretical results [10, 12], it is found that the calculated energy gap for perfectly surface-passivated Si nanoparticles with mean diameter less than about 2 nm without oxygen contamination agree well with the resonance energy in the present PLE spectra and the result of photoemission spectrum in the vicinity of Fermi level of the present *n*-butyl-passivated Si nanoparticles. Therefore, it is concluded that the present strong ultraviolet-blue PL originates from the intrinsic quantum confinement effect and the modified electronic structure due to the intrinsic quantum confinement effect is directly confirmed by the present photoemission spectrum in the vicinity of Fermi level.

4 Summary

We have carried out the various spectroscopic studies of n-butyl-passivated Si nanoparticles with crystalline nature and well n-butyl-passivated surface synthesized by the solution routes. It is found that maximum PL spectrum of n-butyl-passivated Si nanoparticle with mean diameter less than about 2 nm exhibits a strong emission around 3.3 eV in photon energy, and maximum PLE spectrum exhibits a distinct resonance around 4 eV in photon energy. Moreover, the monotonic shifts of PL as a function of excitation energy and PLE as a function of emission energy were observed. From the photoemission spectrum using synchrotron radiation, the detailed valence-band structure of the present n-butyl-passivated Si nanoparticle is clarified, and the valence-band maximum (HOMO) energy was estimated to about 2 eV below the Fermi level. From the comparison of optical spectra (PL and PLE spectra) and photoemission spectrum in the vicinity of Fermi level, it is concluded that the present ultraviolet-blue PL originates from the electron-hole pair recombination between the modified conduction-band (LUMO) and valence-band (HOMO) due to the intrinsic quantum size effect.

This work was supported by Grant-in-Aids from the Ministry of Education, Culture, Sports, Science and Technology of Japan. This work was also supported by the grants from Hyogo Science and Technology Association and Kawanishi Memorial Shinmaywa Education Foundation. Synchrotron-radiation experiment was performed under the Joint Studies Program (2004 and 2005) of the Institute for Molecular Science. We thank T. Ito, S. Kimura, and the staffs of UVSOR-II Facility, Institute for Molecular Science, for their technical support. We also thank S.M. Kauzlarich and K.A. Pettigrew of Department of Chemistry, University of California, Davis, for useful discussions.

References

1. For example, A. Tanaka, S. Onari, T. Arai, Phys. Rev. B **47**, 1237 (1993)
2. For example, L.T. Canham, Appl. Phys. Lett. **57**, 1046 (1990)
3. M. Neyfeh, N. Barry, J. Therrine, O. Akcakir, E. Gratton, G. Bourianoff, Appl. Phys. Lett. **78**, 1131 (2001)
4. R. Gago, L. Vazquez, R. Cuerno, M. Varela, C. Ballesteros, J.M. Albella, Appl. Phys. Lett. **78**, 4028 (2001)
5. X. Wu, A. Bek, A.M. Bittner, Ch. Eggs, Ch. Ossadnik, S. Veprek, Thin Solid Films **425**, 175 (2003)
6. Y.Q. Wang, R. Smirani, G.G. Ross, F. Schiettekatte, Phys. Rev. B **71**, 161310 (2005)
7. X.G. Li, Y.Q. He, M.T. Swihart, Langmuir **20**, 4720 (2004)
8. A. Tanaka, R. Saito, T, Kamikake, M. Imamura, H. Yasuda, Solid State Commun. **140**, 400 (2006)
9. T. Miyadera, A. Koma, T. Shimada, Surf. Sci. **526**, 177 (2003)
10. A. Puzder, A.J. Williamson, J.C. Grossman, G. Galli, Phys. Rev. Lett. **88**, 097401 (2002)
11. K.A. Pettigrew, Q. Liu, P.P. Power, S.S. Kauzlarich, Chem. Mater. **15**, 4005 (2003)
12. F.A. Reboredo, G. Galli, J. Phys. Chem. B **109**, 1072 (2005)